Influence of excitonic oscillator strengths on the optical properties of GaN and ZnO

E. Mallet,[1,2,*] F. Réveret,[1,2] P. Disseix,[1,2] T. V. Shubina,[3] and J. Leymarie[1,2]
[1]*Clermont Université, Institut Pascal (IP), BP 10448, F-63000 Clermont-Ferrand, France*
[2]*Centre National de la Recherche Scientifique, Unité Mixte de Recherche 6602, IP, F-63171 Aubière, France*
[3]*Ioffe Physical-Technical Institute, St. Petersburg 194021, Russia*
(Received 5 February 2014; revised manuscript received 25 April 2014; published 14 July 2014)

We report on an extensive study of the excitonic properties of GaN and ZnO bulk samples with an accurate determination of excitonic parameters by linear and nonlinear spectroscopies. The in-depth comparative study is carried out between these two competitive wide band gap semiconductors for a better understanding of damping processes. In GaN, it is shown that due to microscopic disorder, such as lattice strain fluctuations, inhomogeneous broadening prevails over homogeneous broadening at low temperature. The opposite situation occurs in ZnO, where the homogeneous broadening dominates due to resonant Rayleigh scattering of exciton polaritons and their interaction with acoustic phonons. This comparative study also allows us to highlight the influence of oscillator strengths on spectrally resolved four-wave mixing and time-integrated four-wave mixing.

DOI: 10.1103/PhysRevB.90.045204 PACS number(s): 78.20.−e, 78.47.nj, 78.55.Cr, 78.55.Et

I. INTRODUCTION

In the past three decades, wide band gap semiconductors, such as gallium nitride (GaN) or zinc oxide (ZnO), have been intensively investigated for their potential applications in new optical devices emitting in the near UV region. The GaN technologies are mature. The first GaN light-emitting diode (LED) and laser diode (LD) were obtained, respectively, in 1994 [1] and 1996 [2]. Nowadays, these devices are produced industrially: they are employed in reading Blu-ray digital versatile discs or more recently in LED bulbs. Concerning ZnO, the first realization of an LED is very recent (2008) [3]. Due to the complexity of achieving p-doping in this semiconductor, it is difficult to achieve industrial production at the present time. Thus, the optoelectronics devices based on GaN (LDs, LEDs, etc.) have an advantage over those of ZnO. However, recent developments in polaritonics have shown that the use of materials such as ZnO or GaN with large oscillator strengths is interesting to obtain a low threshold coherent light-emitter at room temperature, namely the polariton laser [4–6]. The latter was observed first by optical pumping in GaN microcavities [7,8] and, more recently, in ZnO [9–12]. For this future device, ZnO presents some advantages (higher oscillator strengths, weak strain sensitivity, etc.), but it has one drawback—the difficulty of obtaining the p-doping. Many studies, however, are being conducted to achieve this doping, and some of them are very promising [13]. Furthermore, an intracavity injection could exclude the need for p-doping. For implementation of these new optical devices based on the exciton polaritons, an in-depth knowledge of the physical properties of both semiconductors is important. Many of these properties have already been fully investigated, such as crystalline structure [14,15], valence band ordering [16,17], photoluminescence (PL) emission [18,19], but no accurate comparative study between these two wide band gap semiconductors is available for their excitonic parameters.

For all these reasons, the aim of this paper is to investigate in detail the near-band-edge optical properties of GaN and ZnO in order to compare these excitonic properties. As in a recent paper [20], accurate information on this subject is deduced here from linear and nonlinear spectroscopies. In addition to continuous wave reflectivity (CW-R), autocorrelation reflectivity (AR), and time-integrated degenerate four-wave mixing (Ti-FWM), already used previously, the spectrally resolved degenerate four-wave mixing (Sr-FWM) experiments are investigated. These nonlinear techniques help us to determine the dephasing time T_2 that reflects polariton interactions with impurities, phonons, and other polaritons [21]. However, Sr-FWM provides additional information [22], namely, the spectral dependence of these interactions. The knowledge of the latter is important to compare GaN and ZnO excitonic behaviors. Finally, the results obtained from all these spectroscopy studies lead to an accurate determination of the excitonic parameters. It is then interesting to compare and understand the different interaction processes involved in both semiconductors.

After a short presentation of the experimental setups and samples, physical models employed in the following are detailed. GaN excitonic parameters are then determined at 5 K from the combination of linear and nonlinear spectroscopies. These results lead naturally to differences between the GaN and ZnO optical properties. We first shall compare their excitonic broadenings, then the beats observed in Ti-FWM spectra will be investigated.

II. EXPERIMENTAL DETAILS

All the experiments were performed on unintentionally doped *c* plane ZnO and homoepitaxial GaN bulk samples. The first one was supplied by Tokyo Denpa Co. and grown by a hydrothermal method, and the second was grown by hydride phase vapor epitaxy. The thickness of these two samples was respectively 1 mm for ZnO and 110 μm for GaN and the overall residual impurity concentration is close to 10^{18} cm^{-3}. The GaN sample (not optimized from the dislocation density point of view) presents a dislocation density slightly inferior to 10^{8} cm^{-2} and a low residual strain. The optical experiments were carried out at low temperature (5 K).

*Corresponding author: emilien.mallet@univ-bpclermont.fr

 ©2014 American Physical Society

Continuous wave reflectivity was performed under normal incidence at 5 K using a xenon lamp for the excitation. Due to the $4f$ optical detection setup, the excitation beam is parallel. The studied area corresponds then to the surface limited by the entrance slit of the spectrometer. The optical signal is analyzed through a monochromator with a 2400 groove/mm grating and detected with a multichannel charge-coupled device (CCD). The spectral resolution obtained with this setup is 0.3 Å.

For the AR experiments at the femtosecond scale, the second-harmonic beam of a femtosecond Ti:sapphire laser with a 110 fs pulse duration and a 76 MHz repetition rate was used. The light pulse is passed through a Michelson interferometer providing two collinear pulses, which are then focused onto the sample. These two pulses are delayed by the time interval τ. The temporal accuracy achieved with the delay line is about 1 fs, and the size spot is equal to 2 mm. The two reflected signals, with an amplitude r, interfere to provide the AR signal. A time-integrated signal is probed as a function of τ by a Si photodiode. The intensity of the time-integrated signal is then given by [23]

$$I_{\mathrm{AR}}(\tau) = 2I_0 + 2C_{rr}(\tau), \tag{1}$$

where I_0 is a constant and $C_{rr}(\tau)$ is the autocorrelation function of reflection amplitude $r(\tau)$.

The Ti-FWM and Sr-FWM setups used the same laser source, detector, and a Michelson interferometer for the time-delay line. The two femtosecond pulses are delayed by the interval time τ but are also spatially translated in this case. They are focused onto the sample using a lens of 0.15 m focal length; hence, the two pulses arrive on the sample with wave vectors $\mathbf{k_1}$ and $\mathbf{k_2}$, and the spot size is equal to 50 μm, which leads to an exciton density close to 10^{16} cm^{-3}. If the $\mathbf{k_1}$ pulse arrives before the $\mathbf{k_2}$ pulse, the delay time τ is positive. The four-wave mixing signal obtained in the $2\mathbf{k_2}$-$\mathbf{k_1}$ direction corresponds to the self-diffraction of $\mathbf{k_2}$ by population grating created by both $\mathbf{k_1}$ and $\mathbf{k_2}$ pulses. When the nonlinear signal is detected by a silicon photodiode, with a slow response time compared to the temporal width pulse, Ti-FWM is recorded; when it is measured through a monochromator with a 2400 groove/mm grating by a fast multichannel CCD, Sr-FWM can be obtained.

III. THEORETICAL CONSIDERATIONS

To analyze AR and CW-R results, knowledge of reflection amplitudes is required. For this, the standard transfer matrix formalism for a multilayered system with planar parallel interfaces has been used. In our case, only three layers will be considered: vacuum, a dead layer with an extension close to the Bohr radius, where no exciton exists, and a semi-infinite medium. The dielectric function is expressed as

$$\varepsilon(E) = \varepsilon_b + \sum_{j=A,B,C} \int_0^{+\infty} \frac{f_j}{E_j^2 - E^2 + i\gamma_j E} \times \exp\left\{-\frac{(x-E_j)^2}{2\sigma_j^2}\right\} dx, \tag{2}$$

with ε_b the background dielectric function derived from ellipsometry measurements [24]. In the above equation, each exciton is characterized by homogeneous broadening γ_j (full width at half maximum), an inhomogeneous broadening σ_j (standard deviation), an oscillator strength $f_j = 4\pi\alpha_{0j}E_j^2$ (with polarizability $4\pi\alpha_{0j}$), and an energy E_j. The index j denotes the exciton A, B, or C.

In the nonlocal model, where inhomogeneous broadening is disregarded, the dielectric function is expressed via [25]

$$\frac{\hbar^2 c^2 k^2}{e^2 E^2} = \varepsilon_b + \sum_{j=A,B,C} \frac{f_j}{E_j^2 - E^2 + \beta_j k^2 + i\gamma_j E}, \tag{3}$$

where $\beta_j = \frac{\hbar^2 E_j}{e M_{\mathrm{exc}\,j}}$ is related to the excitonic dispersion ($M_{\mathrm{exc}\,j}$ is the excitonic mass).

The Ti-FWM and Sr-FWM spectra are analyzed using a model derived from the optical Bloch equation related to the three-level system [26–28], which comprises two excitons (two excited levels and one ground state), denoted here as j and k. Only signals for positive delays are analyzed, so biexcitonic effects are not included. Coulombian interactions are neglected; the longitudinal time T_1^j of the j oscillator is specified to be larger than the transversal one T_2^j, and rotating-wave approximation is assumed. In this framework, the third-order polarization $P^{(3)}(\tau,t)$ calculated for positive delay in the $2\mathbf{k_2}$-$\mathbf{k_1}$ direction for the homogeneous broadening, is given in a short pulse limit (Dirac pulse) by [27]

$$\begin{aligned} P^{(3)}_{\mathrm{hom}}(\tau,t,\omega_j,\omega_k) &= iNM_j^2\left\{2M_j^2 e^{-i\omega_j(t-2\tau)} e^{-\frac{t}{T_2^j}} + M_k^2 e^{-i\omega_j(t-\tau)} e^{-\frac{(t-\tau)}{T_2^j}} e^{i\omega_k\tau} e^{-\frac{\tau}{T_2^k}}\right\} H(t-\tau) \\ &+ iNM_k^2\left\{2M_k^2 e^{-i\omega_k(t-2\tau)} e^{-\frac{t}{T_2^k}} + M_j^2 e^{-i\omega_k(t-\tau)} e^{-\frac{(t-\tau)}{T_2^k}} e^{i\omega_j\tau} e^{-\frac{\tau}{T_2^j}}\right\} H(t-\tau), \end{aligned} \tag{4}$$

where N is the density of a three-level system, M_j and M_k are transition dipole moments associated with the j and k excitons, ω_j,ω_k denote the respective resonance pulsation, and T_2^j,T_2^k correspond to the dephasing times of these excitons. The dephasing time and homogeneous broadening are linked by the relation: $\gamma_j = \frac{2\hbar}{T_2^j}$. The H function is the Heaviside function. For the calculation, the density N is not considered because it is a constant term, while the moments M_j and M_k depend on the oscillator strengths.

The inhomogeneous broadening is now taken into account by integrating the third-order polarization given by Eq. (4) over a two-dimensional Gaussian distribution as [28]

$$P^{(3)}_{\mathrm{inh}}(\tau,t) = \int_0^{+\infty}\int_0^{+\infty} g(\omega_j,\omega_k) P^{(3)}_{\mathrm{hom}}(\tau,t,\omega_j,\omega_k) d\omega_j d\omega_k. \tag{5}$$

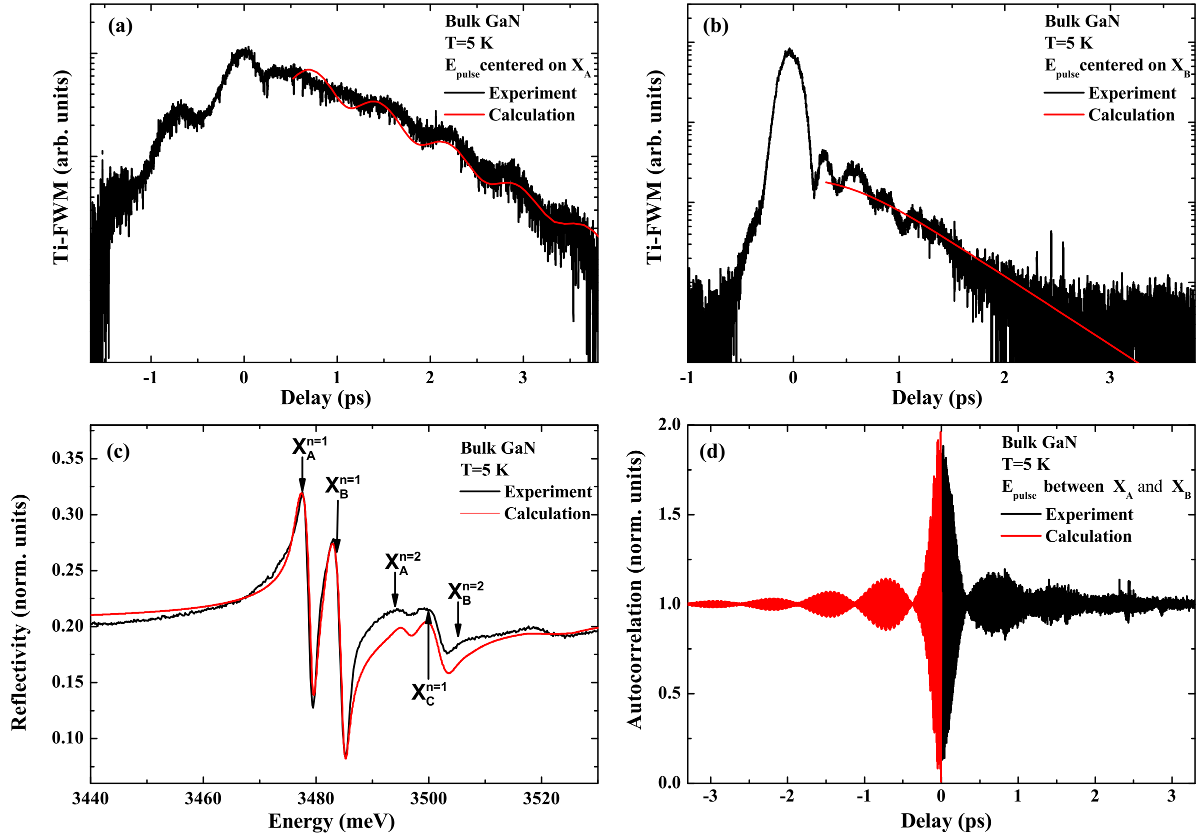

FIG. 1. (Color online) Ti-FWM signal (black lines) recorded in a GaN bulk sample with a pulse central energy corresponding to (a) *A* exciton and (b) *B* exciton resonances. The red lines present the calculation done using Eq. (7). (c) CW-R spectrum (black line) of the GaN bulk sample recorded under normal incidence at 5 K. The red line displays the CW-R simulation using a Gaussian local model. (d) AR spectrum (black line) measured with a pulse energy centered between *A* and *B* excitons. The red line shows the simulation. All measurements were carried out at 5 K.

Here, $g(\omega_j,\omega_k)$ is the distribution function given by

$$g(\omega_j,\omega_k) = \frac{1}{\pi\sigma_j\sigma_k}\exp\left\{-\left[\frac{(\omega_j-\omega_j^c)^2}{2\sigma_j^2}+\frac{(\omega_k-\omega_k^c)^2}{2\sigma_k^2}-\lambda\frac{(\omega_j-\omega_j^c)(\omega_k-\omega_k^c)}{\sigma_j\sigma_k}\right]\right\}, \quad (6)$$

where σ_j and σ_k are inhomogeneous broadenings of j and k excitons, λ is the correlation parameter, which is taken to be equal to unity in our case, ω_I and ω_j are integration variables, ω_j^c and ω_k^c corresponding to the central frequency of resonance pulsations.

The Ti-FWM intensity is given by the following relation obtained from Eq. (5)

$$I_{\text{Ti-FWM}}(\tau) = \int_0^{+\infty}\left|P_{\text{inh}}^{(3)}(t,\tau)\right|^2 dt, \quad (7)$$

where Sr-FWM signal is evaluated from the Fourier transform of Eq. (5):

$$I_{\text{Sr-FWM}}(\tau,\omega) = \left|\int_0^{+\infty} P_{\text{inh}}^{(3)}(t,\tau)e^{-i\omega t}\,dt\right|^2. \quad (8)$$

IV. RESULTS AND DISCUSSION

A. Gallium nitride excitonic parameters

In order to compare zinc oxide with gallium nitride, an accurate knowledge of excitonic parameters is required. Concerning ZnO, the determination of these parameters was obtained previously from an original method combining linear and nonlinear spectroscopies [20]. In the case of GaN, some refinements of this method have been carried out. For Ti-FWM experiments, two spectra are recorded: one with an energy pulse centered on *A* exciton [Fig. 1(a)] and the other on *B* exciton [Fig. 1(b)]. This can be achieved because, contrary to the case of ZnO, the dephasing time of the *B* resonance is larger than the temporal width of the pulse. Thus, the dephasing time of *A* and *B* excitons can be determined separately, and not only the average value, as in the case of ZnO.

The measurement of Ti-FWM decay time τ_{dec} for *A* and *B* excitons leads to the homogeneous broadening, respectively, $\gamma_A = 0.6$ meV and $\gamma_B = 1.1$ meV, when only homogeneous

TABLE I. Excitonic parameters of GaN and ZnO deduced at 5 K from the combination of linear and nonlinear spectroscopies. The values obtained in GaN by Stępniewski *et al.* [31] are also reported.

		Oscillator strength (meV^2)	Polarizability	γ (meV)	σ (meV)	Energy (meV)
GaN						
This work	*XA*	40 000	$3.3*10^{-3} \pm 0.2*10^{-3}$	0.4	0.8	3478.1
	XB	39 000	$3.2*10^{-3} \pm 0.2*10^{-3}$	0.65	0.8	3483.5
Stępniewski	*XA*	—	$2.7*10^{-3} \pm 0.3*10^{-3}$	0.7	—	3476.7
et al. [31]	*XB*	—	$3.1*10^{-3} \pm 0.3*10^{-3}$	1.5	—	3481.5
ZnO	*XA*	155 000	$1.4*10^{-2} \pm 0.1*10^{-2}$	0.55	0.20	3375.2
	XB	250 000	$2.2*10^{-2} \pm 0.1*10^{-2}$	1.35	0.25	3380.7

damping is assumed ($\gamma = \hbar/\tau_{\text{dec}}$). However, these parameters do not allow us to fit the CW-R spectrum. When the broadening is assumed to be mainly inhomogeneous ($\sigma \gg \gamma$.), the decay time derived from the Ti-FWM signal leads to the following homogeneous linewidths $\gamma_A = 0.3$ meV and $\gamma_B = 0.55$ meV and much larger values for inhomogeneous ones ($\gamma = \hbar/2\tau_{\text{dec}}$). These two sets of values limit the range of available values for σ and γ. By considering the intermediate case, where the broadening mechanism is neither purely homogeneous nor mainly inhomogeneous, through Eqs. (2) and (7), the excitonic parameters are adjusted to fit both Ti-FWM [Figs. 1(a) and 1(b)] and CW-R [Fig. 1(c)] spectra. The best fitting parameters are listed in Table I. As the oscillations are not well accounted by the calculations, we have chosen to not include the quantum beats (QBs) in the simulation. The dead layer of 20 Å is used for the simulation of the CW-R spectra. In order to refine the oscillator strength value determination, AR is employed, because the contrast of AR beatings strongly depends on the oscillator strength value. The good agreement between the experimental and calculated data [Fig. 1(d)] is a strong support for the validity of the oscillator strength values that have been determined.

In this previous analysis, the local model [Eq. (2)] has been exclusively used to account for the experimental observations. It was done because, to the best of our knowledge, a rigorous theoretical treatment of the excitonic inhomogeneous broadening within the nonlocal model has not been yet published.

In our previous publication related to ZnO, the measurement of the longitudinal-transverse (LT) splitting of *A* exciton in PL spectra ($\Delta_{\text{LT}}^{A} = 1.5$ meV) has also been used to confirm the oscillator strength values. In the case of the GaN sample,

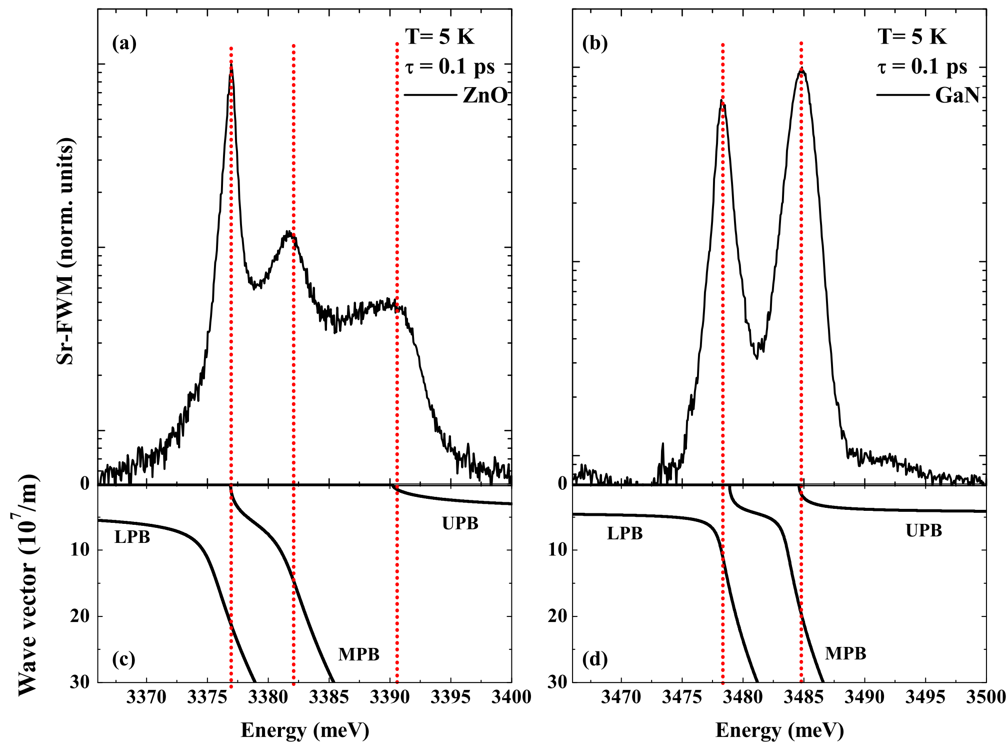

FIG. 2. (Color online) ZnO (a) and GaN (b) Sr-FWM recorded at 5 K. The pulse energy is centered between *A* and B exciton energies. For a better understanding of the peak position, the polariton dispersion curves of ZnO and GaN are plotted on (c) and (d), respectively (see text for details).

the PL signal at the excitonic energy is too weak, and it was not possible to measure any LT splitting value [29] (Δ_{LT}^{A} = 0.8 meV) [30]. However, the comparison with literature [31] (Table I) allows us to confirm the order of magnitude of the oscillator strengths. In fact, we note minor differences between the GaN values reported by Stępniewski *et al.* [31] and our data. Concerning the broadening, the model used by Stępniewski *et al.* [31] is purely homogeneous and does not consider inhomogeneous broadening. Nevertheless, the dissymmetry between *A* and *B* excitonic broadening values is still preserved.

The excitonic parameters determined for ZnO and GaN are compared in Table I. It appears that GaN oscillator strengths are smaller than those of ZnO and that no dissymmetry is observed between the oscillator strengths of *A* and *B* excitons. However, a dissymmetry between the linewidths of *A* and *B* transitions has been found in both ZnO and GaN, being much weaker in the latter than in the former. This dissymmetry will be discussed in the following section dedicated to the interplay between the oscillator strengths and the broadening.

B. Influence of oscillator strength on the excitonic broadening

Examination of Table I shows that at low temperature, the inhomogeneous broadening dominates for GaN, whereas the homogeneous one is predominant in ZnO. The GaN inhomogeneous damping was attributed to the inhomogeneous distribution of the lattice strain [32,33], while ZnO homogeneous broadening was assigned to exciton interactions with impurities or phonons [20]. In order to clarify this difference, Sr-FWM was employed. In Figs. 2(a) and 2(b), Sr-FWM spectra recorded at 5 K at a delay time of 0.1 ps are presented, respectively, for ZnO and GaN. The energy of the pulse was chosen to excite simultaneously the *A* and *B* excitons. The corresponding polariton dispersion curves for each material are plotted [Figs. 2(c) and 2(d)]. Note that the plots of the dispersion are only qualitative; no damping was considered within the nonlocal model [25] given by Eq. (3). The Sr-FWM

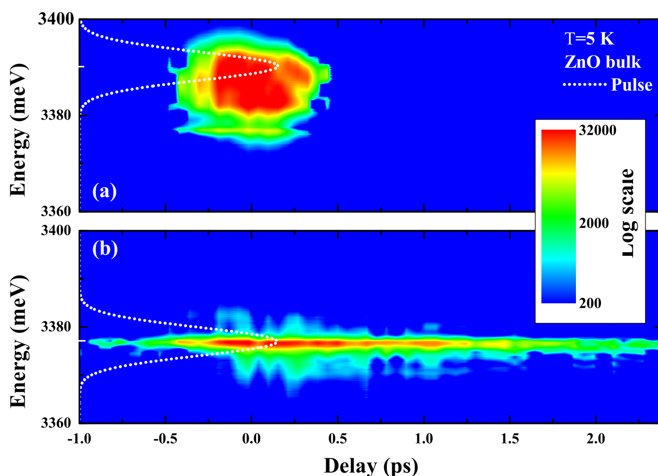

FIG. 3. (Color online) Sr-FWM spectra of ZnO recorded at 5 K with a pulse energy centered on *B* and *A* resonance [Figs. 2(a) and 2(b), respectively]. The dephasing time is larger for the *A* transition. The temporal resolution is 0.06 ps.

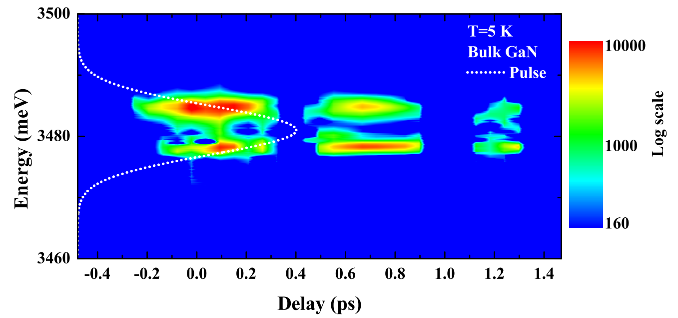

FIG. 4. (Color online) Sr-FWM spectra of GaN recorded at 5 K with a pulse energy centered between the *A* and *B* excitonic resonances.

peak positions are determined by two competitive factors [34]: (i)the strong light-matter coupling achieved near the light line in the dispersion and (ii) the high density of states obtained at the excitonlike dispersion. In the case of ZnO, three peaks are present, whereas only two peaks are detected for GaN. Concerning ZnO, it seems that the lower energy peak corresponds to a mixing between the lower polariton branch (LPB) and the middle polariton branch (MPB), when the latter is near the *A* exciton energy (*A*-MPB). The second peak corresponds to the MPB when it tends to *B* exciton energy (*B*-MPB), and the last one is related to the upper polariton branch (UPB). In the case of GaN, the lower energy peak is the mixing between LPB and *A*-MPB, while the second peak is the mixing between *B*-MPB and UPB. The existence of three peaks for ZnO and only two peaks for GaN can be explained by the difference of the oscillator strength values. In GaN, due to the lower oscillator strength (compared to ZnO), the energy difference between LPB and *A*-MPB is small, and only one peak is observed. This remark also concerns *B*-MPB and UPB, which provide only one peak. In ZnO, the higher oscillator strength values combined with the closeness in energy of *A* and *B* resonances lead to a dissymmetry between the LPB and *A*-MPB splitting and *B*-MPB and UPB, as shown in Fig. 2(c). Small LPB and *A*-MPB splitting induces one peak in Sr-FWM spectra as in GaN, while the large *B*-MPB and UPB splitting leads to the observation of two peaks in Sr-FWM spectra (the ZnO case). Thus, these facts confirm that with lower oscillator strength values or with small splitting only one peak is observed, whereas two peaks are detected for high oscillator strengths. Note that a similar situation has already been reported for $In_xGa_{1-x}As/In_yAl_{1-y}As$ multiple quantum wells [35].

TABLE II. Parameters used for the estimation of the broadening due to the potential deformation interaction. υ_{LA} and D_c-D_υ denote, respectively, the sound velocity for longitudinal waves and the difference between the deformation potential of the conduction band and the valence band [41–45].

	Density (kg.m^{-3})	υ_{LA} (m.s^{-1})	D_c-D_υ (eV)
GaN	6150	7.96*10^3	−6.9
ZnO	5676	6.07*10^3	−3.5

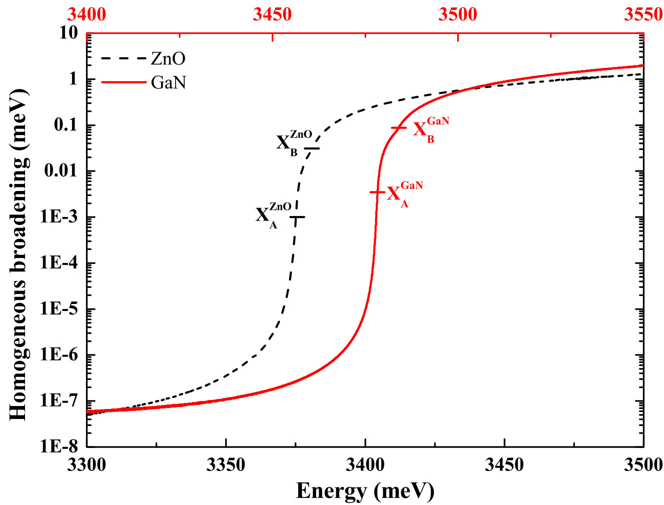

FIG. 5. (Color online) Estimation of the evolution of the homogeneous broadening due to the exciton-acoustic phonon interaction through the deformation potentials in ZnO and GaN.

Concerning the influence of the broadening on the Sr-FWM spectrum of ZnO [Fig. 2(a)], it appears that the broadening increases with the peak energy. This result is consistent with the excitonic parameters deduced from the fit of the Ti-FWM and CW-R spectra (Table I), namely, the broadening of the *B* exciton is larger than that of the *A* exciton. The same evolution can be observed for GaN [Fig. 2(b)]. Sr-FWM spectra of ZnO are displayed as a function of the delay in Fig. 3 for two excitation pulse energies. Figure 3(a) corresponds to the Sr-FWM results obtained with a pulse tuned at the *B* polariton energy, whereas Fig. 3(b) corresponds to those recorded with a pulse centered on the lower polariton mode. In the case of Fig. 3(b), the decay of the four-wave mixing signal is observed only for the *A* polariton mode. Concerning Fig. 3(a), both polaritons are visible, but the *A* polariton is only slightly excited. Due to the weak excitation of the *A* resonance, the intensity of a Sr-FWM signal is also weak and quickly masked by the background signal. However, it can be observed that the dephasing time corresponding to the upper polariton mode is shorter than the dephasing time related to the *A* polariton. This observation has to be associated with the larger broadening of the upper polariton mode compared to that of the *A* polariton. For GaN [Fig. 2(b)], an increase of the damping at the peak energy is also observed. Sr-FWM images for different delays were also recorded, and these results are presented in Fig. 4. The *A* and *B* polaritons are almost equally excited, and the decay of the *B*-related signal appears to be a little faster confirming the results obtained in Sec. IV A.

In order to explain the linewidth dissymmetry at low temperature, various scattering mechanisms have been previously proposed. Among these mechanisms, exciton-exciton

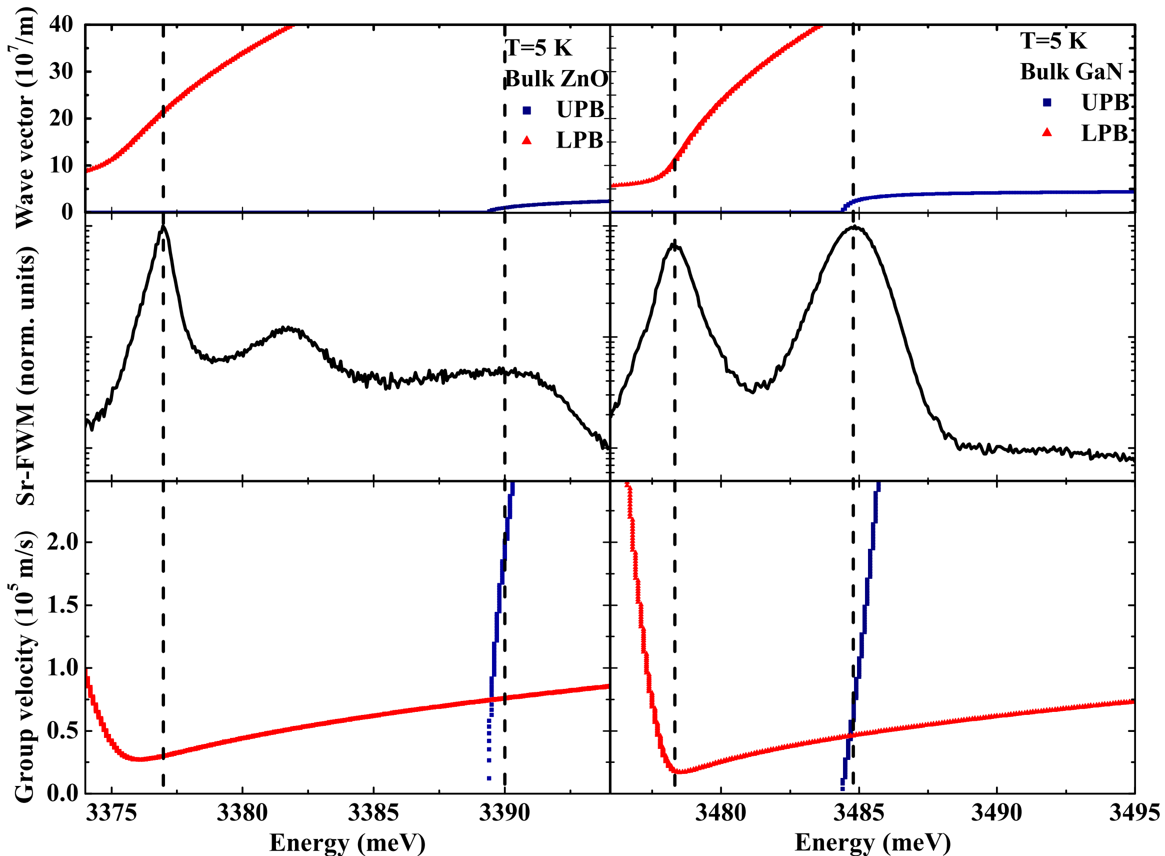

FIG. 6. (Color online) Polariton dispersion curves (LPB and UPB) of ZnO (left side) and GaN (right side) are shown at the top of the figure. In the middle, Sr-FWM spectra of ZnO (left) and GaN (right) are displayed. At the bottom, the polariton group velocity deduced from dispersion is reported. For each semiconductor, the Sr-FWM peaks at lower energy are associated with a slow group velocity. For clarity, the MPBs are not shown in these figures.

scattering [36] can be omitted in our study due to our experimental conditions characterized by weak excitation densities. Indeed, no decrease of the linewidth was observed, when excitation density was decreased. Another mechanism concerns the polariton-acoustic phonon scattering that contributes to the linewidth [37,38], which allowed us to interpret the energy dependence of the damping of exciton-polaritons in CdS crystals [39]. Using the model of Pantke and Broser [39; see Eqs. (4) and (5) of this reference], we performed calculations to estimate the homogeneous part of the broadening due to polariton scattering by acoustic phonons at 0 K. Only the deformation-potential interaction was taken into account, because the contribution of the piezoelectric effect is small [40], below the longitudinal frequency. Parameters used for these calculations were found in the literature [41–45] and summarized in Table II. The damping evolution as a function of energy is plotted in Fig. 5 (red solid line for ZnO and black dashed line for GaN). The influence of the excitonic polariton-acoustic phonon scattering on the damping is weak at low energy (typically at the A exciton resonance energy). On the high energy side (near the B exciton resonance), the damping is, however, more important. So, a certain dissymmetry between both polaritons can be induced by this interaction. At the same time, this effect as a function of energy should be similar in both ZnO and GaN. Thus, it cannot explain the difference in the homogeneous broadenings of these two semiconductors as a function of energy alone.

Another possible damping process in these compounds is the exciton-impurity scattering that has already been reported [46–49]. For GaN samples, Wang *et al.* [48] have investigated the influence of the impurity concentration on damping. The conclusion of their study is that the contribution of exciton-impurity scattering to the broadening is non-negligible. In the immediate vicinity of an excitonic resonance, the damping due to the exciton polariton-impurity interactions can be described by the following expression [49]

$$\Gamma_{\text{exc-imp}} \equiv N_{\text{imp}}\sigma_{\text{eff}} v_g. \tag{9}$$

Here, N_{imp} is the impurity density, and σ_{eff} is the scattering cross section and the polariton group velocity $v_g(E) = \hbar^{-1} dE/dk$. For a given material, the broadening versus energy evolution can be affected by the group velocity modification. The latter is calculated for the upper and LPBs using a nonlocal model and neglecting damping, as a function of energy for each material (Fig. 6). In the case of ZnO, the variation of group velocity is substantial, and the group velocity corresponding to the LPB peak energy differs largely from that related to the UPB peak. The same holds true for GaN; however, this difference appears to be weaker. The origin of this dissimilarity in the velocity variation is obviously associated with the different oscillator strengths. Higher oscillator strengths in ZnO contribute to an increase of the group velocity, which has to be correlated with an increase of the exciton-impurity scattering in accordance with Eq. (9). Thus, the scattering with impurities can explain the increase of linewidth with energy through the polaritonic dispersion.

Thanks to Sr-FWM experiments, the origin of excitonic homogeneous broadening at low temperature can be clarified for both semiconductors. It turns out to be that the exciton polariton-acoustic phonon interaction and, more significantly, the exciton-polariton-impurity scattering contribute to the homogenous broadening; the latter contributes to an increase of the homogeneous broadening versus peak energy and also induces the larger homogeneous linewidth dissymmetry in ZnO with respect to GaN. We note that the consideration presented here is only phenomenological, but it is sufficient

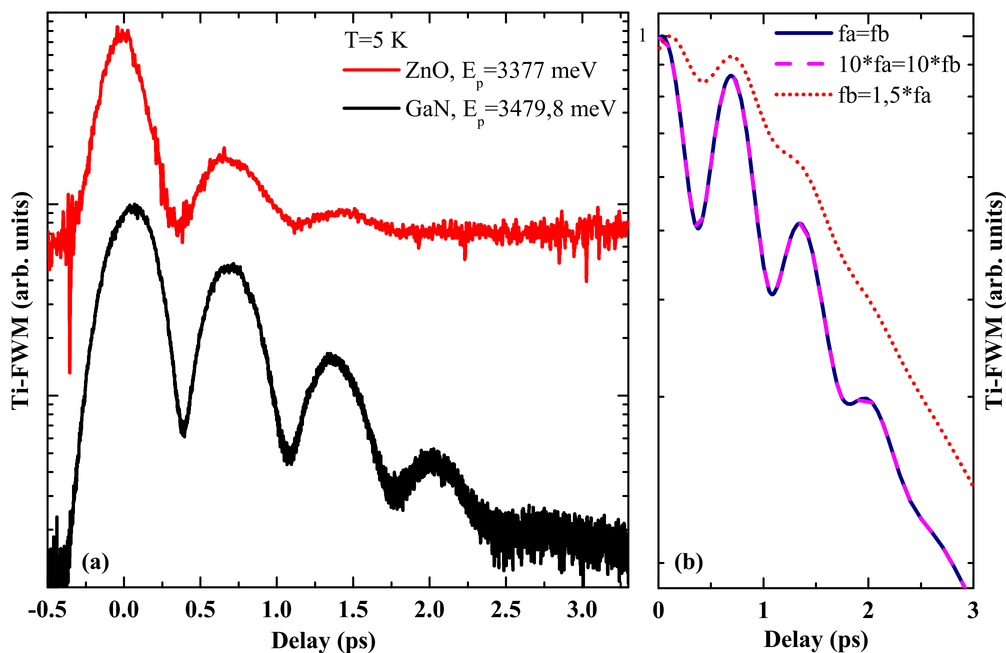

FIG. 7. (Color online) (a) Low temperature (5 K) Ti-FWM signal of ZnO (red line) and GaN (black line). (b) The solid blue line and dashed pink line correspond to the calculation of the Ti-FWM with the A oscillator strength equal to the B one. The blue line corresponds to oscillator strengths ten times smaller than the pink one. In order to compare beat contrast, the two spectra are normalized. The red dotted line corresponds to the calculation where the oscillator strength of B is 1.5 larger than the A one.

to explain the increase of the homogeneous broadening versus energy for a given material. To compare these two materials, a more elaborate model should be developed.

In the following section, the influence of the oscillator strength on the QBs observed in Ti-FWM will be analyzed. These beats arise from the coherent superposition of two excitonic levels simultaneously excited by the femtosecond pulse, whose spectral width is larger than the splitting energy between two excitonic transitions.

C. Influence of oscillator strengths on Ti-FWM and AR QBs

In Fig. 7(a), Ti-FWM spectra recorded for a pulse energy centered between the A and B polaritons are plotted for both ZnO (red line) and GaN (black line). For the sake of clarity, the spectra have been normalized. Obviously, QBs are more pronounced in the case of GaN than for ZnO. This behavior could again be explained by examining the oscillator strengths. Basically, two reasons can be assumed:

(i) The important discrepancy between the oscillator strength values of ZnO and GaN that is almost one order of magnitude between these two semiconductors.

(ii) The dissymmetry between A and B oscillator strengths that is distinctly pronounced in ZnO.

Each of these assumptions is tested by changing the oscillator strengths values in the numerical simulations [Eq. (7)]. All the results are displayed in Fig. 7(b). As previously mentioned, the calculated spectra have been normalized with respect to the zero delay value for comparison. It is clearly shown that only the oscillator strength discrepancy between the A and B excitons affects the contrast of beats. In the case of the lower discrepancy as in GaN, when almost equal resonances are interacted, the QBs have higher amplitude and are prolonged. The lower QB contrast in ZnO, in comparison to GaN, is then ascribed to the higher asymmetry in the interacting resonances.

V. CONCLUSION

Through an investigation of excitonic parameters using linear and nonlinear spectrocopies, the main differences between GaN and ZnO have been highlighted. Two bulk samples of high quality have been thoroughly investigated. A factor of 4 to 7 between ZnO and GaN oscillator strength values is observed; it depends on the exciton that is considered. In contrast to ZnO, no significant discrepancy between the A and B excitonic oscillator strengths in GaN is reported within the experimental error bars. A difference concerning the broadening nature at low temperature between these two wide band gap semiconductors is also emphasized. In GaN, inhomogeneous damping appears to be the dominant process due to lattice strain fluctuations, while homogeneous broadening predominates in ZnO.

Furthermore, a linewidth increase versus excitonic peak energy is demonstrated by Sr-FWM measurements, which corroborate the results derived from the analysis of the CW-R and Ti-FWM spectra. This more pronounced increase for ZnO is enhanced by the dissymmetry between the A and B excitonic oscillator strengths. Finally, the comparison of the Ti-FWM spectra recorded for both semiconductors shows the influence of oscillator strength on the QBs.

ACKNOWLEDGMENTS

The authors thank M. Gallart for his helpful discussions. We also acknowledge support from GaNEX (Grant No. ANR-11-LABX-0014). GaNEX belongs to the publicly funded "investissements d'avenir" program managed by the French National Research Agency. T.V.S. appreciates the support of the Russian Foundation for Basic Research (Grant No. 13-02-00801).

[1] S. Nakamura, T. Mukai, and M. Senoh, Appl. Phys. Lett. **64**, 1687 (1994).
[2] S. Nakamura, M. Senoh, S.-i. Nagahama, N. Iwasa, T. Yamada, T. Matsushita, H. Kiyoku, and Y. Sugimoto, Jpn. J. Appl. Phys. **35**, L74 (1996).
[3] S. Chu, M. Olmedo, Z. Yang, J. Kong, and J. Liu, Appl. Phys. Lett. **93**, 181106 (2008).
[4] A. Kavokin and B. Gil, Appl. Phys. Lett. **72**, 2880 (1998).
[5] G. Malpuech, A. Di Carlo, A. Kavokin, J. J. Baumberg, M. Zamfirescu, and P. Lugli, Appl. Phys. Lett. **81**, 412 (2002).
[6] M. Zamfirescu, A. Kavokin, B. Gil, G. Malpuech, and M. Kaliteevski, Phys. Rev. B **65**, 161205(R) (2002).
[7] S. Christopoulos *et al.*, Phys. Rev. Lett. **98**, 126405 (2007).
[8] G. Christmann, R. Butté, E. Feltin, J. F. Carlin, and N. Grandjean, Appl. Phys. Lett. **93**, 051102 (2008).
[9] T. Guillet *et al.*, Appl. Phys. Lett. **99**, 161104 (2011).
[10] F. Li *et al.*, Phys. Rev. Lett. **110**, 196406 (2013).
[11] H. Franke, C. Sturm, R. Schmidt-Grund, G. Wagner, and M. Grundmann, New J. Phys. **14**, 013037 (2012).
[12] L. Orosz *et al.*, Phys. Rev. B **85**, 121201(R) (2012).
[13] E. H. Khan, M. H. Weber, and M. D. McCluskey, Phys. Rev. Lett. **111**, 017401 (2013).
[14] C. F. Klingshirn, B. K. Meyer, A. Waag, A. Hoffmann, and J. M. M. Geurts, *Zinc Oxide: From Fundamental Properties towards Novel Applications* (Springer, Berlin, 2010).
[15] B. Gil, *Low-Dimensional Nitride Semiconductors* (Oxford University Press, New York, 2002).
[16] A. V. Rodina, M. Strassburg, M. Dworzak, U. Haboeck, A. Hoffmann, A. Zeuner, H. R. Alves, D. M. Hofmann, and B. K. Meyer, Phys. Rev. B **69**, 125206 (2004).
[17] R. Dingle, D. D. Sell, S. E. Stokowski, and M. Ilegems, Phys. Rev. B **4**, 1211 (1971).
[18] B. K. Meyer, J. Sann, S. Eisermann, S. Lautenschlaeger, M. R. Wagner, M. Kaiser, G. Callsen, J. S. Reparaz, and A. Hoffmann, Phys. Rev. B **82**, 115207 (2010).
[19] K. Kornitzer, T. Ebner, K. Thonke, R. Sauer, C. Kirchner, V. Schwegler, M. Kamp, M. Leszczynski, I. Grzegory, and S. Porowski, Phys. Rev. B **60**, 1471 (1999).
[20] E. Mallet, P. Disseix, D. Lagarde, M. Mihailovic, F. Réveret, T. V. Shubina, and J. Leymarie, Phys. Rev. B **87**, 161202(R) (2013).

[21] T. Yajima and Y. Taira, J. Phys. Soc. Jpn. **47**, 1620 (1979).
[22] W. Schäfer, D. S. Kim, J. Shah, T. C. Damen, J. E. Cunningham, K. W. Goossen, L. N. Pfeiffer, and K. Köhler, Phys. Rev. B **53**, 16429 (1996).
[23] M. Born and E. Wolf, *Principles of Optics,* 2nd ed. (Pergamon Press, New York, 1964).
[24] M. Mihailovic, A.-L. Henneghien, S. Faure, P. Disseix, J. Leymarie, A. Vasson, D. A. Buell, F. Semond, C. Morhain, and J. Zùñiga Pérez, Opt. Mater. **31**, 532 (2009).
[25] J. J. Hopfield and D. G. Thomas, Phys. Rev. **132**, 563 (1963).
[26] J. Erland and I. Balslev, Phys. Rev. A **48**, R1765 (1993).
[27] J. Erland, K. H. Pantke, V. Mizeikis, V. G. Lyssenko, and J. M. Hvam, Phys. Rev. B **50**, 15047 (1994).
[28] S. T. Cundiff, Phys. Rev. A **49**, 3114 (1994).
[29] T. V. Shubina, A. A. Toropov, G. Pozina, J. P. Bergman, M. M. Glazov, N. A. Gippius, P. Disseix, J. Leymarie, B. Gil, and B. Monemar, Appl. Phys. Lett. **99**, 101108 (2011).
[30] It cannot be concluded that the A exciton oscillator strength of ZnO is twice that of GaN from the factor 2, which exists between the LT splittings (E_{LT}) of A excitons related to ZnO and GaN. Indeed, the relation $f = 2E_0\varepsilon_B E_{LT}$ does apply only for a single exciton and is no more valid when two kinds of excitons (A, B) are close in energy. See C. F. Klingshirn, *Semiconductor Optics* (Springer, Berlin, 2007).
[31] R. Stępniewski, K. P. Korona, A. Wysmolek, J. M. Baranowski, K. Pakula, M. Potemski, G. Martinez, I. Grzegory, and S. Porowski, Phys. Rev. B **56**, 15151 (1997).
[32] O. Aoude, P. Disseix, J. Leymarie, A. Vasson, M. Leroux, E. Aujol, B. Beaumont, A. Trassoudaine, and Y. Andre, Phys. Rev. B **77**, 045206 (2008).
[33] S. Chichibu, H. Okumura, S. Nakamura, G. Feuillet, T. Azuhata, T. Sota, and S. Yoshida, Jpn. J. Appl. Phys. **36**, 1976 (1997).
[34] H. Tahara, M. Bamba, Y. Ogawa, and F. Minami, Phys. Rev. B **86**, 235208 (2012).
[35] T. Rappen, G. Mohs, and M. Wegener, Phys. Rev. B **47**, 9658 (1993).
[36] S. Pau, J. Kuhl, F. Scholz, V. Haerle, M. A. Khan, and C. J. Sun, Phys. Rev. B **56**, R12718 (1997).
[37] W. C. Tait and R. L. Weiher, Phys. Rev. **166**, 769 (1968).
[38] W. C. Tait and R. L. Weiher, Phys. Rev. **178**, 1404 (1969).
[39] K. H. Pantke and I. Broser, Phys. Rev. B **48**, 11752 (1993).
[40] S. Rudin, T. L. Reinecke, and B. Segall, Phys. Rev. B **42**, 11218 (1990).
[41] A. Segura, J. A. Sans, F. J. Manjon, A. Munoz, and M. J. Herrera-Cabrera, Appl. Phys. Lett. **83**, 278 (2003).
[42] T. B. Bateman, J. Appl. Phys. **33**, 3309 (1962).
[43] B. K. Meyer *et al.*, Phys. Status Solidi B **241**, 231 (2004).
[44] O. Ambacher *et al.*, J. Phys.: Condens. Matter **14**, 3399 (2002).
[45] K. Kim, W. R. L. Lambrecht, and B. Segall, Phys. Rev. B **53**, 16310 (1996).
[46] M. Dagenais and W. F. Sharfin, Phys. Rev. Lett. **58**, 1776 (1987).
[47] E. Vanagas, J. Kudrna, D. Brinkmann, P. Gilliot, and B. Hönerlage, Phys. Rev. B **63**, 153201 (2001).
[48] Y. J. Wang, R. X. Wang, G. Q. Li, and S. J. Xu, J. Appl. Phys. **106**, 013514 (2009).
[49] T. Takagahara, Phys. Rev. B **31**, 8171 (1985).